

Noggin Combined With Dental Pulp Stem Cells Repair Muscle Injury Through Smad/Pax7 Signaling Pathway

Meng-Han Zhang

Shanghai Stomatological Hospital, Fudan University

Li-Ming Yu

Shanghai Stomatological Hospital, Fudan University

Wei-Hua Zhang

Shanghai Stomatological Hospital, Fudan University

Jia-Jia Deng

Shanghai Stomatological Hospital, Fudan University

Bing-Jing Sun

Shanghai Stomatological Hospital, Fudan University

Mei-Hua Chen

Shanghai Stomatological Hospital, Fudan University

Wei Huang

Shanghai Key Laboratory of Craniomaxillofacial Development and Diseases, Fudan University

Hua He

Third Affiliated Hospital of Second Military Medical University

Xin-Xin Han

Shanghai Key Laboratory of Craniomaxillofacial Development and Diseases, Fudan University

Yue-Hua Liu (✉ liyuehua@fudan.edu.cn)

Fudan University <https://orcid.org/0000-0003-3033-8873>

Research

Keywords: Noggin, Dental pulp stem cells, Satellite cells, Matrigel, Volumetric muscle loss

Posted Date: September 8th, 2021

DOI: <https://doi.org/10.21203/rs.3.rs-861400/v1>

License: © ⓘ This work is licensed under a Creative Commons Attribution 4.0 International License.

[Read Full License](#)

Abstract

Background: A proper stem cell source is key to muscle injury repair. Dental pulp stem cells (DPSCs) are an available source for the treatment of muscle injury due to their high reproductive and differential activities. However, the application of DPSCs in muscle regeneration is incompletely understood. Noggin, a secreted BMP antagonist promoted by Wnt-1, is required for embryonic myogenesis. Our research is to study whether Noggin can promote myogenic differentiation of DPSCs, and then to investigate the repair effect of Noggin combined with DPSCs in muscle injury.

Methods: DPSCs were treated with Noggin to induce myogenic differentiation in vitro. The levels of myogenic markers (MyoD, Desmin, MRF4 and MyHC), and satellite cell markers (Pax3, Pax7, Six1 and Eya2) were detected during this process. Next, we blocked the effect of Noggin by adding BMP, and Smad phosphorylation level was tested. Then, we implanted Noggin-pretreated DPSC combined Matrigel into the mouse tibialis anterior muscle with volumetric muscle loss (VML). After 30-day recovery, morphometric analysis of the tibialis anterior muscle was performed.

Results: Noggin effectively increased myotube formation in DPSCs. We also found Noggin accelerated the skeletal myogenic differentiation of DPSCs and promote Pax7+ satellite-like cell generation. These satellite-like cells had the capacity to generate myofibers and could self-renew. Pax7 and Pax3 levels were repressed when blocked the effect of Noggin by adding BMP, and Noggin eliminated the level of BMP/Smad phosphorylation. This suggested that Noggin facilitated the skeletal myogenic differentiation of DPSCs via Smad/Pax7 pathway. Morphometric analysis of muscle cross-sections revealed that DPSCs therapy could increase repair size and decrease scar tissue in tibialis anterior muscle of VML. Moreover, Noggin-treated DPSCs can benefit to Pax7+ satellite cell pool and promote muscle regeneration.

Conclusions: This work reveals that Noggin can promote the generation of satellite-like cells for the myogenic process in DPSCs through Smad/Pax7 signaling pathway, and these satellite-like cells bioconstructs might possess a relatively fast capacity to regenerate for muscle injury.

Introduction

Muscle stem cells, also called satellite cells (SCs) and defined by the transcription factor paired box 7 (Pax7), are responsible for skeletal muscle maintenance and repair. Once activated after injury, SCs enter cell cycle, commit to myogenic progenitor cells (MPCs), differentiate into myoblast cells, and finally fuse to multinucleated myotubes. A subset of SCs undergoes asymmetric division, renewing the satellite cell pool [1]. However, endogenous SCs may be inefficient in response to severe trauma or chronic degenerative diseases such as malnutrition, neuromuscular diseases and sleep apnea [2–4]. When more than 20% of the muscle volume is missing, as in volumetric muscle loss (VML), endogenous self-repair is hindered [5]. Moreover, SCs are found in very limited number in adult muscles and exhibit undesirable amplification activity in vitro [6]; thus, these SCs are not the appropriate stem cell pool for muscle repair.

Dental pulp stem cells (DPSCs) are a type of mesenchymal stem cells that exhibit therapeutic potential for tissue regeneration [7]. DPSCs possess the ability to undergo skeletal myogenic differentiation, and the resulting myogenic lineage cells could be used to treat the dystrophic muscles of mdx/SCID mice [8]. However, the ideal conditions for myogenic induction have not been clarified. Here, we searched for novel factors to develop appropriate skeletal myogenic differentiation systems for DPSCs.

Noggin, a secreted homodimeric glycoprotein, was discovered to induce secondary axis formation in *Xenopus* embryos [9]. Noggin is modestly expressed in mesoderm-derived tissues and required for embryonic somite and skeletal patterning [10]. Then, Noggin was found to inhibit the actions of bone morphogenetic protein (BMP)-2, -4, -5, -7, -13 and -14, thus blocking Smad-dependent signaling [11]. BMP signaling has been shown to play a role in controlling satellite cell lineage progression during embryonic myogenesis [12], and these satellite cell progeny secrete BMP antagonists, such as Noggin, for the differentiation of muscle progenitor cells [13]. Noggin-null mice display serious skeletal defects [14]. However, the effect of Noggin on skeletal myogenic differentiation and adult muscle repair has not yet been reported.

Based on these observations, DPSCs have been explored for myogenic differentiation and widely demonstrated to have great therapeutic potential for muscle injury [8]. Although several methods to modify these stem cell cultures to make better use of regenerative myogenesis have been introduced, the efficiency of this process is quite low. Therefore, based on the previews strategy, Noggin were introduced to apply modification on skeletal myogenic differentiation systems for DPSCs. Then we implanted these pretreated DPSCs into the mouse tibialis anterior muscle with VML to verify the repair capacity of the DPSCs in muscle injury. In this study, we explore the possibility of obtaining muscle stem cells from Noggin-pretreated DPSCs, subsequently helping to provide a source of cells for muscle repair.

Materials And Methods

Cell culture and identification

DPSCs were acquired as previously described (Fig. S1A-B, Table S1) [15] and cultured with α -MEM (Gibco, NY, USA) supplemented with 10% fetal bovine serum (FBS, Gibco, NY, USA) and 1% penicillin-streptomycin (Gibco, NY, USA) at 37°C in the presence of 5% CO₂ and 95% air. Flow cytometric analysis was used to determine the cell surface markers present on hDPSCs. hDPSCs were identified with phycoerythrin (PE)-conjugated antibody against human CD29 (#555443) and FITC-conjugated antibody against human CD90 (#555595) from BD Biosciences (CA, USA), fluorescein isothiocyanate (FITC)-conjugated antibody against human CD44 (#11-0441-85) from eBioscience (CA, USA), and PE-conjugated antibody against human CD34 (#343605) and FITC-conjugated antibody against human CD45 (#304005) from BioLegend (CA, USA) and analyzed using FlowJo software (FlowJo, OR, USA). Cell cycle analysis was also performed after staining for 24 h with propidium iodide (PI) (Beyotime, Shanghai, China) according to the manufacturer's protocol using flow cytometry (ACEA NovoCyte, CA, USA).

Myogenic differentiation assay

DPSCs were seeded on 6-well plates at a cell density of 4000 cells/cm² in expansion medium consisting of α -MEM supplemented with 10% FBS for adherence. When the confluence reached 80%, the culture medium was replaced first with myogenic induction medium containing the following for 24 h: IMDM (Gibco, NY, USA) + 2% FBS + 1 μ M 5-Aza (Sigma-Aldrich, CA, USA) [16]. IMDM + 2% FBS without 5-Aza served as the base control medium. Subsequently, cells were rinsed three times in phosphate-buffered saline (PBS, HyClone, UT, USA) and then transferred to the following differentiation medium: IMDM with 10% FBS (defined as day 0) (Fig. 1a). The differentiation medium was supplemented with or without Noggin (100 ng/ml or 200 ng/ml) or 50 ng/ml BMP4. Noggin (#10267) from Sino Biological (Beijing, China) and BMP4 (HZ-1045) from HumanZyme (IL, USA) were used. Cells were cultured for 3 weeks, the differentiation medium was changed every 3 days, and the cells were observed under a microscope to confirm the formation of myotubes.

VML defect modeling and stem cell transplantation

Animal protocols were approved by the Animal Ethics Committee of Fudan University. Male Balb/C mice (8 weeks old) were purchased from Shanghai Bikai Biotechnology. All animals were given surgery to generate a muscle defect with unilateral resection of the tibialis anterior muscle under 10% chloral hydrate anesthesia. The thin layer of fascia covering the tibialis anterior muscle was dissected away, and a 2×5 mm area was stained by hematine. After blunt separation, a 2 mm-deep cut was made around the stained hematine, creating a 2×5×2mm defect. This VML defect accounted for a loss of approximately 40% of the tibialis anterior muscle. DPSCs were cultured and differentiated into satellite-like cells with 5-aza and Noggin treatment, and Matrigel (Corning, NY, USA) was used to provide a scaffold for stem cell transplant. Matrigel alone (n = 6) or Matrigel combined with Noggin-treated (n = 6) or untreated DPSCs (n = 6) was used to fill the dissected area. If no immediate transplantation was performed (n = 6), the incision was sutured closed. Mice were allowed to heal for 30 days.

Hematoxylin and Eosin Staining

The tibialis anterior muscles were excised from mice in the four groups and fixed in ice-cold 4% PFA. After dehydration in a graded alcohol series, the tissue was embedded in paraffin and cut into 5 μ m-thick sections by using a Leica RM2255 rotary microtome (Leica Microsystems, Mannheim, Germany). After deparaffinization in xylene and hydration through a graded alcohol series to ddH₂O, hematoxylin and eosin (Servicebio, Wuhan, China) staining was performed according to the manufacturer's protocols.

RNA Extraction and Real-Time Polymerase Chain Reaction (PCR)

Total RNA was extracted from the cells using TRIzol (Life Technologies, CA, USA). The RNA concentration was quantified using a spectrophotometer by measuring the OD_{260/280} ratio (1.80–1.95). cDNA was reverse transcribed using a FastQuant RT Kit (Tiangen, Beijing, China) according to the manufacturer's protocol. Subsequently, quantitative PCR was performed using SYBR Green Premix (Tiangen, Beijing,

China) on a Light Cycler 96 system (Roche, Basel, Switzerland) with each primer at 0.6 mM and 150 ng of cDNA template. Transcript levels were normalized to β -actin levels, which acted as a control. The primer sequences can be found in Supplementary Table 2.

Western Blot Analysis

Total protein was extracted in RIPA lysis buffer (Thermo Fisher Scientific, MA, USA) plus protease/phosphatase inhibitor cocktail (#5872, CST, MA, USA). Lysate proteins (25 mg) were loaded on SDS-polyacrylamide gels (7.5% or 10%) and then transferred onto PVDF membranes. Target proteins on the membranes were incubated overnight at 4 °C with primary antibodies diluted 1:1000–1:200 in 1× TBS-Tween (TBS: 0.05 M Tris, 0.15 M NaCl (pH 7.5); with 0.2% Tween-20). Antibodies against β -actin (abs830031; Absin Bioscience, Shanghai, China), Pax7 (ab187339) and Myf5 (ab125078) from Abcam, MyHC IIB (BF-F3) and MyHC IIA (SC-71) from Developmental Studies Hybridoma Bank (DSHB, ID, USA); p-Smad 1/5/9 (#13820) and Smad 1 (#6944) from Cell Signaling Technology (CST, MA, USA); MyoD1 (#18943), Desmin (#60226), MRF4 (#11754), Pax3 (#21383), Six1 (#10709), Eya2 (#11314), ID1 (#18475) and MSX1 (#17678) from Proteintech (IL, USA) were used. After intensive washing, the membranes were incubated with HRP-conjugated secondary antibodies (#7076, anti-mouse IgG; #7074, anti-rabbit IgG, both from CST) for 1–2 h. The membranes were visualized using Super Signal West Dura substrate (Thermo Scientific, MA, USA), and the bands were detected with an AI600 imager (GE Healthcare, IL, USA).

Immunofluorescence microscopy

Cells, myofibers, and sections were fixed with 4% paraformaldehyde and placed in PBS containing 0.25% Triton X-100 for 10 min. After blocking with 3% bovine serum albumin (BSA, Solarbio, Beijing, China) in PBS for 30 min at room temperature, they were then incubated with primary antibody in PBS containing 2.5% BSA at 4 °C overnight. In addition to the primary antibodies listed above, antibodies against Pax7 (PAX7, DSHB), CD34 (#14486, Proteintech), human LaminA/C (MBS477941, MyBioSource), human Nucleoli (ab190710, Abcam) and Laminin (ab11575, Abcam) were used. After washing, the samples were incubated with anti-mouse-Alexa-594, or -488 or anti-rabbit-Alexa-594, or -488 (Jackson ImmunoResearch, PA, USA) and then 4',6-diamidino-2-phenylindole (DAPI). Images of the cells were captured by a microscope (Leica Microsystems, Mannheim, Germany) and analyzed by ImageJ.

Statistical analysis

We performed statistical analyses using GraphPad Prism 5.0. Data are expressed as the mean \pm standard deviation. The protein quantifies were analyzed by semiquantitative analysis. Comparison between groups was performed by Mann-Whitney *U* test or Kruskal-Wallis *H* test with multiple comparison. Statistical significance was defined as * $p < 0.05$, ** $p < 0.01$, *** $p < 0.001$.

Results

Noggin promotes the formation of myotubes in DPSCs

The effective myogenic differentiation of stem cells is crucial for their repair of muscle injury. 5-Aza-2'-deoxycytidine (5-Aza) might be important for triggering the myogenic commitment of DPSCs. According to the results of Pisciotta et al., DPSCs cultured in the absence of preliminary 5-Aza treatment did not show any labeling for myogenic-specific markers, even when cultured in myogenic induction medium [8]. Therefore, we cultured and identified DPSCs (Fig. S1A-D) and found that 5-Aza induced myotube formation in DPSCs with an increase in myogenic markers (Fig. S2A-E). In the same field of vision, a relatively smaller number of myotubes that appeared to exhibit atrophy formed. However, 5-Aza-induced myogenic differentiation still showed low efficiency.

Noggin, a secreted BMP antagonist derived from the notochord and somite, is believed to improve myogenesis on epaxial somite [17]. To examine whether Noggin could affect the myogenic differentiation of DPSCs, we treated DPSCs with Noggin after 5-Aza induction (Fig. 1A). First, we found that Noggin had no effect on the cell proliferation of DPSCs (Fig. S3A-C) but increased myotube formation in the DPSCs (Fig. 1B-C). A more pronounced myotube morphology was observed after treatment with the Noggin protein for 21 days, and the number of multinuclear myotubes increased significantly (Fig. 1D). myosin heavy chain (MyHC) (Fig. 1E), such as MyHCIIA (Fig. 1F) and MyHCIIB (Fig. 1G) were significantly increased compared with those in the control group. This finding implies that Noggin might facilitate the formation of myotubes in DPSCs.

Noggin accelerates the progression of skeletal myogenic differentiation in DPSCs

Several myogenic genes, such as myogenic differentiation 1 (MyoD1), myogenic regulatory factor 4 (MRF4) and Desmin, have been proven to regulate myogenic processes, including myoblast differentiation into myocytes, fusion into myotubes and maintenance of the integrity of muscle cells [18, 19]. Therefore, we assessed the expression of MyoD1, MRF4 and Desmin on day 7, 14 and 21. The increased mRNA expression of MyoD1 (Fig. 2A) and Desmin (Fig. 2B) compared with that in the control group began on the seventh day. Noggin increased expression of MyoD1 and Desmin (Fig. 2A, B) but had no effect on the mRNA expression of MRF4 on day 7 (Fig. 2C). Immunofluorescence staining for MyoD1 (Fig. 2D) and Desmin (Fig. 2E) showed increased levels of MyoD1 (Fig. 2F) and an increased number of long, spindle-shaped myotube-like cells in Noggin-treated groups (Fig. 2G). On day 14, the increased protein expression of MyoD1 was also observed, indicating myoblast production [18]. In contrast, on day 21, MyoD1 expression decreased with disappeared trend (Fig. 2H, I). Our results were verified by an earlier study showing that secreted Noggin facilitated MyoD expression in embryonic tissues [20]. Moreover, the protein expression levels of Desmin (Fig. 2J) and MRF4 (Fig. 2K) were also significantly increased upon treatment with Noggin (Fig. 2H). In our study, Noggin has been shown to play an important regulatory role in accelerating the skeletal myogenic differentiation of DPSCs, which might be a novel factor in myogenesis.

The generation of satellite-like cells in DPSCs and their asymmetric self-renewal capacity

MPCs during development and SCs in adults are characterized by expression of paired box (Pax)3/7 [21]. SIX homeobox 1 (Six1) and EYA transcriptional coactivator and phosphatase 2 (Eya2) activate SCs (Pax7+) [22, 23], and the Six1-Eya2 complex functions in MPC specification by acting upstream of Pax3 and Myf5 expression and promoting myoblast differentiation [24, 25]. Thus, we measured the relative mRNA levels of Pax7, Pax3, Six1 and Eya2 on day 1, 3, and 7 as well as the protein expression levels of Six1, Pax3, Pax7 and Eya2 on day 7, 14 and 21.

The mRNA expression of Pax7 began to increase on day 1, increased in a concentration-dependent manner until peaking on day 3, and remained higher level compared to control on day 7 (Fig. 3A). Consistent with the expression of Pax7, the mRNA expression of Pax3 was increased on day 3, and remained increased on day 7 (Fig. 3B), and the mRNA expression of Six1 (Fig. 3C) and Eya2 (Fig. 3D) was increased on day 7. Western blotting (Fig. 3E) and immunofluorescence staining (Fig. 3F) for Pax7 showed that Noggin upregulated the protein expression of Pax7 on day 7, 14 and 21 (Fig. 3G, H). The protein expression levels of Pax3 (Fig. 3I), Six1 (Fig. 3J) and Eya2 (Fig. 3K) were also increased in the Noggin-treated groups on day 14 and remained high on day 21 (Fig. 3E). Previous studies have concluded that Pax3-mediated myogenesis requires an environment in which Six1 synergizes with Eya2 to activate the expression of MyoD [24, 26]. Our results showed that Noggin promoted the expression of Six1 and Eya2, suggesting that these Pax3/7 + cells were under such an environment for subsequent myogenic differentiation.

To address the functional significance of Six1/Eya2 expression in satellite-like cells, we compared our sequential expression data with that from other studies. Chang et al. introduced Pax7 + satellite-like cells from mES cells and found an earlier appearance of Pax3 expression on day 3, followed by Pax3/Pax7 expression on day 10, with the expression of Pax3 stronger than that of Pax7 [27]. In our study, we found that with Noggin treatment, the protein expression of Pax7 was at a high level on day 7 and Pax3/Six1/Eya2 expressions were increased on day 14 and 21 (Fig. 3E, H-K). One possible explanation for this difference is that hDPSCs went through an initial wave of differentiation into myogenic precursor cells that expressed Pax7 to promote myotube formation, followed by a second wave of differentiation into cells expressing Pax3/Six1/Eya2. This explanation implies that Noggin promotes the myogenic process in hDPSCs through upregulating the expression of members of the Pax3/Six1/Eya2 axis in addition to Pax7.

Noggin facilitates the skeletal myogenic differentiation of DPSCs via Smad/Pax7 pathway

As described before, Noggin is an antagonist of BMP. Cao et al. reported that BMP-4 appeared to inhibit myogenic differentiation of bone marrow-derived mesenchymal stromal cells by suppressing the transcriptional activity of myogenic factors [28]. To determine whether Noggin regulates the myogenic differentiation of DPSCs by regulating BMP signaling, we first simulated 3D protein structures using SWISS-MODEL and visualized them with PyMOL software, which showed that Noggin competitively inhibits the binding of BMP4 to BMP-receptor I A (BMPRIA) (Fig. 4A). Then, we blocked the effect of Noggin by adding the BMP protein. The protein levels of Pax7, Pax3, Eya2, MyoD1, and Desmin were

observed (Fig. 4B). Compared with Noggin treatment (200N), the expression decreased in Noggin + BMP treatment. Among them, Pax3 and Pax7 was most obvious when compared with 5-Aza or control groups.

To further explore downstream regulation of BMP signaling by Noggin, the phosphorylation levels of members of the BMP/p-Smad pathway were also detected (Fig. 4C-E). The protein levels of p-Smad 1/5/9 were increased after activation of the BMP pathway by adding BMP4 (Fig. 4C). Noggin persistent eliminated the phosphorylation levels at 3h, 6h, and 9h even subsequently stimulated with BMP4 (Fig. 4C-E). The downstream effectors of the BMP/p-Smad pathway, such as inhibitor of DNA binding 1 (ID1) and msh homeobox 1 (MSX1) were also downregulated by Noggin treatment (Fig. 4F-J). Consistent with our results, studies have also shown that ID1 and MSX1 can restrict myogenic gene expression, and impeded myoblast differentiation [29, 30]. Therefore, our results indicated that Noggin facilitates the skeletal myogenic differentiation of DPSCs via Smad/Pax7 pathway.

Noggin-pretreated DPSCs combined Matrigel can effectively repair muscle injury in VML

To test the utility of DPSCs in repairing muscle injury, we established a mouse VML injury model that accounted for a loss of approximately 40% of the tibialis anterior muscle (Fig. 5A-C). In the untreated VML-injured group, the volumetric defect remained (Fig. 5D, top panel, large dotted blackline). Shrinkage resulting from the defect area occurred. The deformity of the muscle defect showed the deposition of a thin layer of disorganized, collagenous scar tissue (Fig. 5D top panel, small dotted purple line). The injury defect exceeded the threshold and could not be restored by the endogenous regenerative potential of the skeletal muscle. This indicated the success of VML modeling. Quarta et al. reported a similar mouse model of VML that resulted in the irrecoverable loss of muscle function and structure. Consistent with our model, peripheral fibrotic scarring was observed in place of the excised muscle and also extended into the belly of muscle [31].

Hydrogel biomaterials are widely used in skeletal muscle regeneration as they provide a structural framework for the delivery of cells or growth factors to damaged muscle [32]. Therefore, we used the thermosensitive hydrogel Matrigel to provide a scaffold for stem cell transplantation (Fig. 5D). We observed that the Matrigel group exhibited a reduced shrinkage area and decreased muscle fibrosis (Fig. 5D, second panel, and Fig. 5D). Sicariet al. reported histological changes in VML muscles treated with a biologic scaffold material at different time points and showed that the defect area was infiltrated with cells during repair [33]. We also found some mononuclear cell infiltrate in the defect (Fig. 5D, second panel, small dotted red line).

To examine whether Noggin-pretreated DPSCs could better repair muscle injury than the control conditions, we transplanted DPSCs bioconstructs into the defects of VML muscles (Fig. 5A-C). Quarta et al. treated VML muscles with hydrogel Matrigel reconstituted muscle stem cells, which resulted in muscle tissue formation and fibrotic infiltration [31]. We implanted Noggin-pretreated or untreated DPSCs reconstituted in Matrigel into the defects. Morphometric analysis of muscle cross-sections revealed that, relative to the untreated DPSCs groups (Fig. 5D, third panel), Noggin-pretreated DPSCs groups showed decreased size of defect and scar tissue (Fig. 5D, bottom panel, and Fig. 5E, F). In contrast to the above

two groups, which showed irreversible and robust fibrotic scars, DPSC-treated defects consisted of markedly reduced fibrotic tissue surrounded by cells of varying morphologies, including fibrotic, inflammatory, and vessel-like cells, indicating the process of tissue repair (Fig. 5D, third panel, small dotted red line). In contrast, Noggin-pretreated DPSCs might have accelerated this process and facilitated the improved formation of muscle tissue, leaving little cell infiltration (Fig. 5D, bottom panel, small dotted red line).

Noggin-pretreated DPSCs can benefit to muscle satellite cell population and promote myogenic repair

To explore the contribution of grafted cells to muscle injury, immunostainings of muscle cross-sections were performed by Pax7 (satellite cell marker), MyoD (activated satellite cells/myoblasts), human Nucleoli (hNu) and human LaminA/C (specific antibody to track human cells), and Laminin (to identify position within the sarcolemma) (Fig. 5G-N). Pax7/MyoD co-staining revealed that stem cell transplantation increased proportion of activated satellite cells when compared with sham or Matrigel groups (Fig. 5G, H). We also observed that hNu was integrated into the nucleus of regenerated tissue and was located on the Laminin-stained muscle sarcolemma (Fig. 5I, white arrow), that was more readily discovered in Noggin-treated DPSCs groups than DPSCs groups. An increased number of hLaminA/C+/Pax7+ (Fig. 5J, left two columns, white arrow) and hNu+/MyoD+ (Fig. 5J, right two columns, purple arrow) cells were also discovered in Noggin-treated DPSCs groups when compare with DPSCs groups, representing increased donor-derived satellite cells (Fig. 5K-N). These results suggested that Noggin-treated DPSCs had partly benefit to satellite cell population. This benefit might offer support to muscle regeneration in VML injury.

Discussion

In our study, we found that Noggin could promote the skeletal myogenic differentiation of DPSCs and increase the generation of satellite-like cells through Smad/Pax7 signaling. Then, we treated VML model mice with Noggin-pretreated DPSCs and found that Noggin pretreatment improved the repair of muscle injury. Our work implies that Noggin can promote the skeletal myogenic differentiation of DPSCs, rendering DPSCs an important source for muscle stem cells in muscle repair.

Previous studies indicated that MyoD-induced myogenic cells from DPSCs could promote muscle regeneration when transplanted into the injured muscles of mice [34]. However, owing to the uncertain risks of using integrated viral vectors to induce genes, researchers are developing novel factors to regulate myogenic differentiation networks.

Understanding the regulatory network of embryonic myogenesis would help to identify such regulators and better explain our research results. Embryonic myogenesis involves complex interplay between signaling molecules secreted surround the somite. For instance, Wnts from the dorsal ectoderm stimulate myogenesis, and BMP4 from the lateral plate mesoderm inhibits myogenesis [35]. A recent RNA-seq analysis identified that BMP signaling pathways are repressed in the transition from the presomitic mesoderm to nascent somites, whereas Wnt signaling was found to be required for both presomitic

mesoderm specification and the transition from nascent somites to developed somites [36]. Chal et al. found that Wnt activation alone can induce pluripotent stem cells committed to Pax3 + progenitors, and further requires BMP inhibition to keep progenitor fate, followed by the myogenic program to generate myotubes and associated Pax7 + cells [37]. This finding suggests that Wnt activation or BMP antagonism might be an important mechanism of myogenesis regulation.

Noggin, a secreted BMP antagonist, was promoted by Wnt-1 in medial somites and found to promote the expression of MyoD in embryonic tissues [38]. Blockade of Wnt signals downregulated Noggin and Myf5 [39]. Therefore, Noggin might be a key protein linker for Wnt and BMP signals during myogenesis. Our results showed that Noggin could promote the skeletal myogenic differentiation of DPSCs. Cao et al. reported that BMP-4 appeared to inhibit myogenic differentiation of bone marrow-derived mesenchymal stromal cells by suppressing the transcriptional activity of myogenic factors [28]. When competing for MSX1, downstream effectors of the BMP/p-Smad pathway increase Pax3 expression in embryonic tissues [40]. Domiziana et al. developed the muscles of *Noggin*^{-/-} mice and found the increased phosphorylation of Smad1/5/8 with concomitant induction of BMP target genes ID1, ID2, and ID3 as well as MSX1, and reduced number of mesenchymal Pax7 + muscle precursor cells [41]. In our study, we found that the myogenic effect could be blocked by the BMP protein via Smad/Pax7 pathway, accompanied by the downregulation of MSX1 and ID1 levels (Fig. 6).

Given that MPCs (Pax3+) are more sensitive than other myogenic cell types to external stimuli, such as BMP signaling, and will later become resident muscle stem cells (also called SCs). After birth, muscle homeostasis is ensured by SCs, which requires the expression of Pax7 [42]. Pax7 + satellite-like cells are characterized by the capacity to generate myofibers and undergo self-renewal [1]. Our study found that after 21 days of differentiation, the expression of late myogenic marker genes, such as MyHC, as well as early myogenic marker genes, such as Pax7, was high under Noggin treatment. This implies that similar to SCs, these modified DPSCs may undergo a period of asymmetric self-renewal. iPSCs could be induced to satellite-like cells, accompanied by MPC specification, following stimulation with the resemble regulators [43]. Chang et al. reported that Pax7 + satellite-like cells from mouse embryonic stem cells had an extensive self-renewal capacity when transplanted into a muscle injury model [27]. LaBarge et al. discovered the possibility that satellite cells from the mesenchymal stem cells of bone marrow give rise to differentiated muscle fibers [44]. Furthermore, Costamagna et al. found that knockdown of Noggin in the mouse muscle reduced the number of mesenchymal Pax7 + muscle precursors [41]. In our study, the results suggested that Noggin could promote the differentiation of satellite-like cells from DPSCs and that these satellite-like cells might have the ability to transform into myogenic precursor cells and facilitate myogenesis (Fig. 6).

To test the effective utility of Noggin in muscle regeneration, therefore, we transplanted Noggin-pretreated DPSCs combined with Matrigel into defects of a VML injury model. Kerkiset al. published a study on the therapeutic effect of immature human DPSCs systemic transplantation into golden retrievers with muscular dystrophy [45]. Researchers have used 5-Aza-induced human amniotic mesenchymal cells to treat rat tibialis anterior muscle defects with VML, with the therapeutic effects of increased angiogenesis

and improved tissue repair [46]. Our results showed that Noggin-pretreated DPSCs possessed an increased capacity for regeneration and reduced scarring during repair.

To further investigate Noggin-pretreated DPSCs in the maintenance and function of muscle SCs, we compared the different types of donor cells for muscle regeneration. Chang et al. reported the successful in vitro induction of Pax7 + satellite-like cells from mouse embryonic stem cells with self-renewal capacity in a subsequent muscle injury model [26]. Some scholars also transplanted ESCs or iPSCs-derived muscle progenitor cells into NSG-*mdx*^{Acv} mice, and found donor-derived LaminAC+/Pax7 + satellite cells in tissues, suggesting the contribution of transplanted cells to muscle stem cell pool [47]. However, Alessandra et al. found the contribution of 5-Aza-induced DPSCs engraftment in dystrophic muscle of *mdx*/SCID mice might be a paracrine effect [8]. Different from muscle-derived or embryonic stem cells, transplant efficiency of mesenchymal stem cells was relatively low, with about 1–2% as hybrid myofibers [48]. Our results indicated that Noggin-treated DPSCs can increase the nuclei fusion rate to about 15–20%. This suggested that Noggin-treated DPSCs can partly benefit to muscle satellite cell pool and promote myogenic repair in VML injury. This suggests the importance of producing Pax7 + SCs and the potential of these SCs for improved muscle regeneration. Noggin might increase the generation of satellite-like cells from DPSCs to provide potential transplantable stem cells for muscle injury. Further improved conditions of induction and transplantation were required to better application of DPSCs.

Conclusions

In summary, Noggin is an important protein that promotes myogenic differentiation and increases the production of satellite-like cells through Smad/Pax7 pathway. These satellite-like cells can effectively repair VML injury. Noggin, a secreted BMP antagonist, is thought to be the target gene of Wnt signaling [49]. This implies that Noggin maybe the link that coordinates both the Wnt and BMP pathways. Recent protocols apply small molecules to direct differentiation towards the myogenic lineage. Chalet al. induced Wnt signaling activation (CHIR99021) and applied inhibitors of BMP signaling (LDN193189) along with promyogenic growth factors, including FGF2, HGF, and IGF, to induce the differentiation of iPSCs or ESCs towards the myogenic lineage [21, 50]. Whether we can use other small molecules to coordinate both the Wnt and BMP pathways, similar to Noggin, may be our next research topic.

Abbreviations

DPSCs: Dental pulp stem cells; VML: Volumetric muscle loss; SCs: satellite cells; Pax: Paired box; MPCs: Myogenic progenitor cells; BMP: Bone morphogenetic protein; 5-Aza: 5-Aza-2'-deoxycytidine; MyHC: Myosin heavy chain; MyoD1: Myogenic differentiation 1; MRF4: Myogenic regulatory factor 4; Six1: SIX homeobox 1; Eya2: EYA transcriptional coactivator and phosphatase 2; BMPRIA: BMP-receptor I; ID1: DNA binding 1; MSX1: msh homeobox 1; 100N: 100 ng/ml Noggin; 200N: 200 ng/ml Noggin; N-DPSCs: Noggin-treated DPSCs; hNu: human Nucleoli

Declarations

Acknowledgements

We thank everyone on our team for assisting with the preparation of this manuscript.

Authors' contributions

YHL and XXH conceived and designed the experiments. MHZ, LMY, WHZ, and JJD performed the experiments. LMY, BJS, MHC, WH, and HH analyzed data and interpreted results. MHZ and WHZ assembled the figures. YHL and XXH provided financial support. MHZ and LMY wrote the manuscript. YHL and XXH reviewed and edited the manuscript. All authors read and approved the final manuscript. MHZ and LMY contributed equally to this work.

Funding

This study was supported by Natural Science Foundation of Shanghai (19ZR1445400), National Natural Science Foundation of China (81771109, 81901031, 82071153).

Availability of data and materials

All supporting data are included in the article and its additional files.

Ethics approval and consent to participate

Animal protocols were approved by Animal Welfare and Ethics Committee of Department of Laboratory Animal Science, Fudan University (ethical number NO. 20171311A692). The research proposal for use of human samples were approved by Medical Ethical Committee of Shanghai Stomatological Hospital, Fudan University.

Consent for publication

Not applicable.

Competing interests

The authors declare that they have no competing interests.

References

1. Chal J, Pourquie O. Making muscle: skeletal myogenesis in vivo and in vitro. *Development* 144 2017;144:2104-2122. <http://doi.org/10.1242/dev.151035>
2. Kalyani RR, Corriere M, Ferrucci L. Age-related and disease-related muscle loss: the effect of diabetes, obesity, and other diseases. *Lancet Diabetes Endocrinol* 2014;2:819-829. [http://doi.org/10.1016/S2213-8587\(14\)70034-8](http://doi.org/10.1016/S2213-8587(14)70034-8)

3. Dong J, Niu X, Chen X. Injury and apoptosis in the palatopharyngeal muscle in patients with obstructive sleep apnea-hypopnea syndrome. *Me Injury and apoptosis in the palatopharyngeal muscle in patients with obstructive sleep apnea-hypopnea syndrome. d. Sci. Monit.* 2020;26:e919501. <http://doi.org/10.12659/MSM.919501>
4. Pollot BE, Corona BT. Volumetric muscle loss. *Methods Mol. Biol.* 2016;1460:19-31. http://doi.org/10.1007/978-1-4939-3810-0_2
5. Garg K, Ward CL, Hurtgen BJ, Wilken JM, Stinner DJ, Wenke JC, et al. Volumetric muscle loss: persistent functional deficits beyond frank loss of tissue. *J. Orthop. Res.* 2015;33:40-46. <http://doi.org/10.1002/jor.22730>
6. Sun C, Serra C, Lee G, Wagner KR. Stem cell-based therapies for duchenne muscular dystrophy. *Exp. Neurol.* 2020;323:113086. <http://doi.org/10.1016/j.expneurol.2019.113086>
7. Kawashima N. Characterisation of dental pulp stem cells: a new horizon for tissue regeneration? *Arch. Oral Biol.* 2012;57:1439-1458. <http://doi.org/10.1016/j.archoralbio.2012.08.010>
8. Pisciotta A, Riccio M, Carnevale G, Lu A, De Biasi S, Gibellini L, et al. Stem cells isolated from human dental pulp and amniotic fluid improve skeletal muscle histopathology in mdx/SCID mice. *Stem Cell Res. Ther.* 2015;6:156. <http://doi.org/10.1186/s13287-015-0141-y>
9. Smith WC, Harland RM. Expression cloning of noggin, a new dorsalizing factor localized to the spemann organizer in xenopus embryos. *Cell* 1992;70:829-840. [http://doi.org/10.1016/0092-8674\(92\)90316-5](http://doi.org/10.1016/0092-8674(92)90316-5)
10. Sharma R, Shafer M, Bareke E, Tremblay M, Majewski J, Bouchard M. Bmp signaling maintains a mesoderm progenitor cell state in the mouse tailbud. *Development* 2017;144:2982-2993. <http://doi.org/10.1242/dev.149955>
11. Brazil DP, Church RH, Surae S, Godson C, Martin F. BMP signalling: agony and antagonism in the family. *Trends Cell Biol.* 2015;25:249-264. <http://doi.org/10.1016/j.tcb.2014.12.004>
12. Stantzou A, Schirwis E, Swist S, Alonso-Martin S, Polydorou I, Zarrouki F, et al. BMP signaling regulates satellite cell-dependent postnatal muscle growth. *Development* 2017;144:2737-2747. <http://doi.org/10.1242/dev.144089>
13. Linker C, Lesbros C, Stark MR, Marcelle C. Intrinsic signals regulate the initial steps of myogenesis in vertebrates. *Development* 2003;130:4797-4807. <http://doi.org/10.1242/dev.00688>
14. Tylzanowski P, Mebis L, Luyten FP. The Noggin null mouse phenotype is strain dependent and haploinsufficiency leads to skeletal defects. *Dev. Dyn.* 2006;235:1599-1607. <http://doi.org/10.1002/dvdy.20782>
15. Zhang W, Yu L, Han X, Pan J, Deng J, Zhu L, et al. The secretome of human dental pulp stem cells protects myoblasts from hypoxia-induced injury via the Wnt/betacatenin pathway. *Int. J. Mol. Med.* 2020;45:1501-1513. <http://doi.org/10.3892/ijmm.2020.4525>
16. Nakatsuka R, Nozaki T, Uemura Y, Matsuoka Y, Sasaki Y, Shinohara M, et al. 5-Aza-2'-deoxycytidine treatment induces skeletal myogenic differentiation of mouse dental pulp stem cells. *Arch. Oral Biol.* 2020;55:350-357. <http://doi.org/10.1016/j.archoralbio.2010.03.003>

17. Marcelle C, Stark MR, Bronner-Fraser M. Coordinate actions of BMPs, Wnts, Shh and noggin mediate patterning of the dorsal somite. *Development* 1997;124:3955-3963.
18. Zammit PS. Function of the myogenic regulatory factors Myf5, MyoD, Myogenin and MRF4 in skeletal muscle, satellite cells and regenerative myogenesis. *Semin. Cell Dev. Biol.* 2017;72:19-32. <http://doi.org/10.1016/j.semcdb.2017.11.011>
19. Roman W, Gomes ER. Nuclear positioning in skeletal muscle. *Semin. Cell Dev. Biol.* 2018;82:51-56. <http://doi.org/10.1016/j.semcdb.2017.11.005>
20. Reshef R, Maroto M, Lassar AB. Regulation of dorsal somitic cell fates: BMPs and Noggin control the timing and pattern of myogenic regulator expression. *Genes Dev.* 1998;12:290-303. <http://doi.org/10.1101/gad.12.3.290>
21. Buckingham M, Relaix F. PAX3 and PAX7 as upstream regulators of myogenesis. *Semin. Cell Dev. Biol.* 2015;44:115-125. <http://doi.org/10.1016/j.semcdb.2015.09.017>
22. Grifone R, Demignon J, Giordani J, Niro C, Souil E, Bertin F, et al. Eya1 and Eya2 proteins are required for hypaxial somitic myogenesis in the mouse embryo. *Dev Biol.* 2007;302:602-616. <http://doi.org/10.1016/j.ydbio.2006.08.059>
23. Wurmser M, Chaverot N, Madani R, Sakai H, Negroni E, Demignon J, et al. SIX1 and SIX4 homeoproteins regulate PAX7+ progenitor cell properties during fetal epaxial myogenesis. *Development* 2020:147. <http://doi.org/10.1242/dev.185975>
24. Maire P, Dos SM, Madani R, Sakakibara I, Viaut C, Wurmser M. Myogenesis control by SIX transcriptional complexes. *Semin. Cell Dev. Biol.* 2020;104:51-64. <http://doi.org/10.1016/j.semcdb.2020.03.003>
25. Ridgeway AG, Skerjanc IS. Pax3 is essential for skeletal myogenesis and the expression of Six1 and Eya2. *J. Biol. Chem.* 2001;276:19033-19039. <http://doi.org/10.1074/jbc.M011491200>
26. Heanue TA, Reshef R, Davis RJ, Mardon G, Oliver G, Tomarev S, et al. Synergistic regulation of vertebrate muscle development by Dach2, Eya2, and Six1, homologs of genes required for Drosophila eye formation. *Genes Dev.* 1999;13:3231-3243. <http://doi.org/10.1101/gad.13.24.3231>
27. Chang H, Yoshimoto M, Umeda K, Iwasa T, Mizuno Y, Fukada S, et al. Generation of transplantable, functional satellite-like cells from mouse embryonic stem cells. *FASEB J.* 2009;23:1907-1919. <http://doi.org/10.1096/fj.08-123661>
28. Jiqing C, Yaqin L, Yingyin L, Fei C, Huili Z, Yuling Z, et al. BMP4 inhibits myogenic differentiation of bone marrow-derived mesenchymal stromal cells in mdx mice. *Cytotherapy* 2015;17:1213-1219. <http://doi.org/10.1016/j.jcyt.2015.06.010>
29. Leng X, Ji X, Hou Y, Settlege R, Jiang H. Roles of the proteasome and inhibitor of DNA binding 1 protein in myoblast differentiation. *FASEB J.* 2019;33:7403-7416. <http://doi.org/10.1096/fj.201800574RR>
30. Zhu X, Li M, Jia X, Hou W, Yang J, Zhao H, et al. The homeoprotein Msx1 cooperates with Pkn1 to prevent terminal differentiation in myogenic precursor cells. *Biochimie* 2019;162:55-65. <http://doi.org/10.1016/j.biochi.2019.04.003>

31. Quarta M, Cromie M, Chacon R, Blonigan J, Garcia V, Akimenko I, et al. Bioengineered constructs combined with exercise enhance stem cell-mediated treatment of volumetric muscle loss. *Nat. Commun.* 2019;8:15613. <http://doi.org/10.1038/ncomms15613>
32. Lev R, Seliktar D. Hydrogel biomaterials and their therapeutic potential for muscle injuries and muscular dystrophies. *J. R. Soc. Interface* 2018;15. <http://doi.org/10.1098/rsif.2017.0380>
33. Sicari BM, Agrawal V, Siu BF, Medberry CJ, Dearth CL, Turner NJ, et al. A murine model of volumetric muscle loss and a regenerative medicine approach for tissue replacement. *Tissue Eng. Part A* 2012;18:1941-1948. <http://doi.org/10.1089/ten.TEA.2012.0475>
34. Sung SE, Hwang M, Kim AY, Lee EM, Lee EJ, Hwang SK, et al. MyoD overexpressed equine adipose-derived stem cells enhanced myogenic differentiation potential. *Cell Transplant* 2016;25:2017-2026. <http://doi.org/10.3727/096368916X691015>
35. Chang CN, Kiousi C. Location, location, location: signals in muscle specification. *J. Dev. Biol.* 2018;6. <http://doi.org/10.3390/jdb6020011>
36. Xi H, Fujiwara W, Gonzalez K, Jan M, Liebscher S, Van Handel B, et al. In vivo human somitogenesis guides somite development from hPSCs. *Cell Rep.* 2017;18:1573-1585. <http://doi.org/10.1016/j.celrep.2017.01.040>
37. Chal J, Al TZ, Oginuma M, Moncuquet P, Gobert B, Miyanari A, et al. Recapitulating early development of mouse musculoskeletal precursors of the paraxial mesoderm in vitro. *Development* 2018;45. <http://doi.org/10.1242/dev.157339>
38. Hirsinger E, Duprez D, Jouve C, Malapert P, Cooke J, Pourquie O. Noggin acts downstream of Wnt and Sonic Hedgehog to antagonize BMP4 in avian somite patterning. *Development* 1997; 124:4605-4614.
39. Tajbakhsh S, Borello U, Vivarelli E, Kelly R, Papkoff J, Duprez D, et al. Differential activation of Myf5 and MyoD by different Wnts in explants of mouse paraxial mesoderm and the later activation of myogenesis in the absence of Myf5. *Development* 1998;125:4155-4162.
40. Daubas P, Duval N, Bajard L, Langa VF, Robert B, Mankoo BS, et al. Fine-tuning the onset of myogenesis by homeobox proteins that interact with the Myf5 limb enhancer. *Biol. Open* 2015;4:1614-1624. <http://doi.org/10.1242/bio.014068>
41. Costamagna D, Mommaerts H, Sampaolesi M, Tylzanowski P. Noggin inactivation affects the number and differentiation potential of muscle progenitor cells in vivo. *Sci. Rep.* 2016;6:31949. <http://doi.org/10.1038/srep31949>
42. von Maltzahn J, Jones AE, Parks RJ, Rudnicki MA. Pax7 is critical for the normal function of satellite cells in adult skeletal muscle. *Proc. Natl. Acad. Sci. U S A* 2013;110:16474-16479. <http://doi.org/10.1073/pnas.1307680110>
43. Chal J, Al TZ, Hestin M, Gobert B, Aivio S, Hick A, et al. Generation of human muscle fibers and satellite-like cells from human pluripotent stem cells in vitro. *Nat. Protoc.* 2016;11:1833-1850. <http://doi.org/10.1038/nprot.2016.110>

44. LaBarge MA, Blau HM. Biological progression from adult bone marrow to mononucleate muscle stem cell to multinucleate muscle fiber in response to injury. *Cell* 2002;111:589-601. [http://doi.org/10.1016/s0092-8674\(02\)01078-4](http://doi.org/10.1016/s0092-8674(02)01078-4)
45. Kerkis I, Ambrosio CE, Kerkis A, Martins DS, Zucconi E, Fonseca SA, et al. Early transplantation of human immature dental pulp stem cells from baby teeth to golden retriever muscular dystrophy (GRMD) dogs: Local or systemic? *J. Transl. Med.* 2008;6:35. <http://doi.org/10.1186/1479-5876-6-35>
46. Zhang D, Yan K, Zhou J, Xu T, Xu M, Lin J, et al. Myogenic differentiation of human amniotic mesenchymal cells and its tissue repair capacity on volumetric muscle loss. *J. Tissue Eng.* 2019;10: 1543350788. <http://doi.org/10.1177/2041731419887100>
47. Darabi R, Arpke R, Irion S, T Dimos J, Grskovic M, Kyba M et al. Human ES- and iPS-derived myogenic progenitors restore DYSTROPHIN and improve contractility upon transplantation in dystrophic mice. *J. Cell stem cell* 2012;10:610-619. <http://doi: 10.1016/j.stem.2012.02.015>.
48. Chretien F, Dreyfus PA, Christov C, Caramelle P, Lagrange JL, Chazaud B, et al. In vivo fusion of circulating fluorescent cells with dystrophin-deficient myofibers results in extensive sarcoplasmic fluorescence expression but limited dystrophin sarcolemmal expression. *Am. J. Pathol.* 2005;166:1741-1748. [http://doi.org/10.1016/S0002-9440\(10\)62484-4](http://doi.org/10.1016/S0002-9440(10)62484-4).
49. Borello U, Coletta M, Tajbakhsh S, Leyns L, De Robertis EM, Buckingham M, et al. Transplacental delivery of the Wnt antagonist Frzb1 inhibits development of caudal paraxial mesoderm and skeletal myogenesis in mouse embryos. *Development* 1999;126:4247-4255.
50. Chal J, Oginuma M, Al TZ, Gobert B, Sumara O, Hick A, et al. Differentiation of pluripotent stem cells to muscle fiber to model Duchenne muscular dystrophy. *Nat. Biotechnol.* 2015;33:962-969. <http://doi.org/10.1038/nbt.3297>

Figures

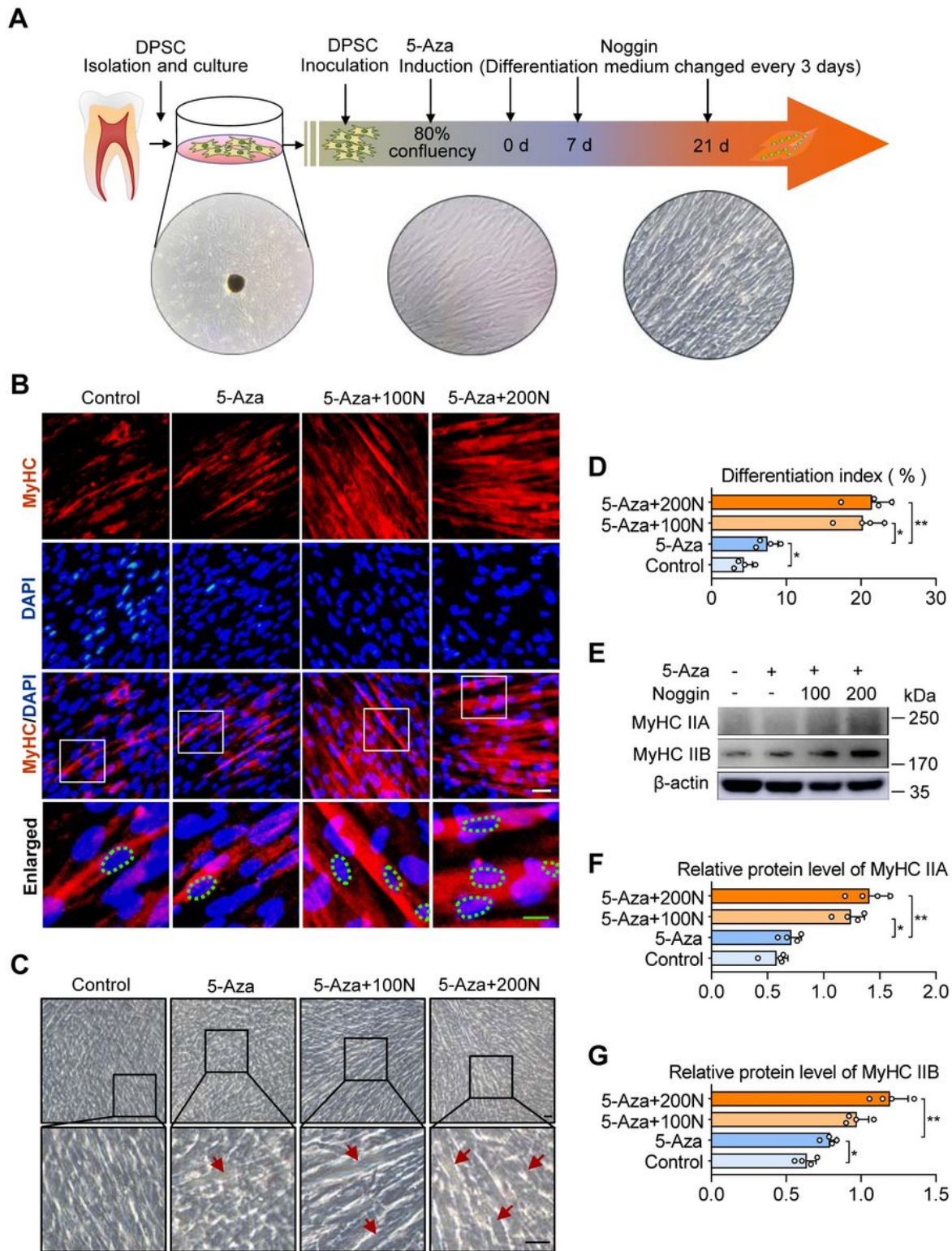


Figure 1

Noggin promotes the formation of myotube in DPSCs. A In vitro myogenic differential system for DPSCs. B Formation of myotubes and cell nuclei was assessed using immunofluorescence staining with MyHC (red) and DAPI (blue) on day 21, respectively. Green dotted circle indicated MyHC positive merged myonuclei; white scale bar, 10 μ m; green scale bar, 5 μ m. C Cell morphology of hDPSCs induced by 5-Aza with or without Noggin (100 ng/ml or 200 ng/ml) after 21 days. Red arrowheads indicated Myotube-like

cells; Scale bar, 50 μ m. D The differentiation index is presented as the ratio of MyHC positive nuclei to total nuclei (n = 4). E Protein expression of MyHC IIA, MyHC IIB was assessed using western blotting on day 21. F-G Semiquantitative analysis of the expression ratio of (F) MyHC IIA/ β -actin, and (G) MyHC IIB/ β -actin (n = 4). The difference between control and 5-Aza or between 5-Aza, 5-Aza + 100N and 5-Aza + 200N were presented as *p < 0.05, **p < 0.01, and ***p < 0.001. 100N = 100 ng/ml Noggin; 200N = 200 ng/ml Noggin.

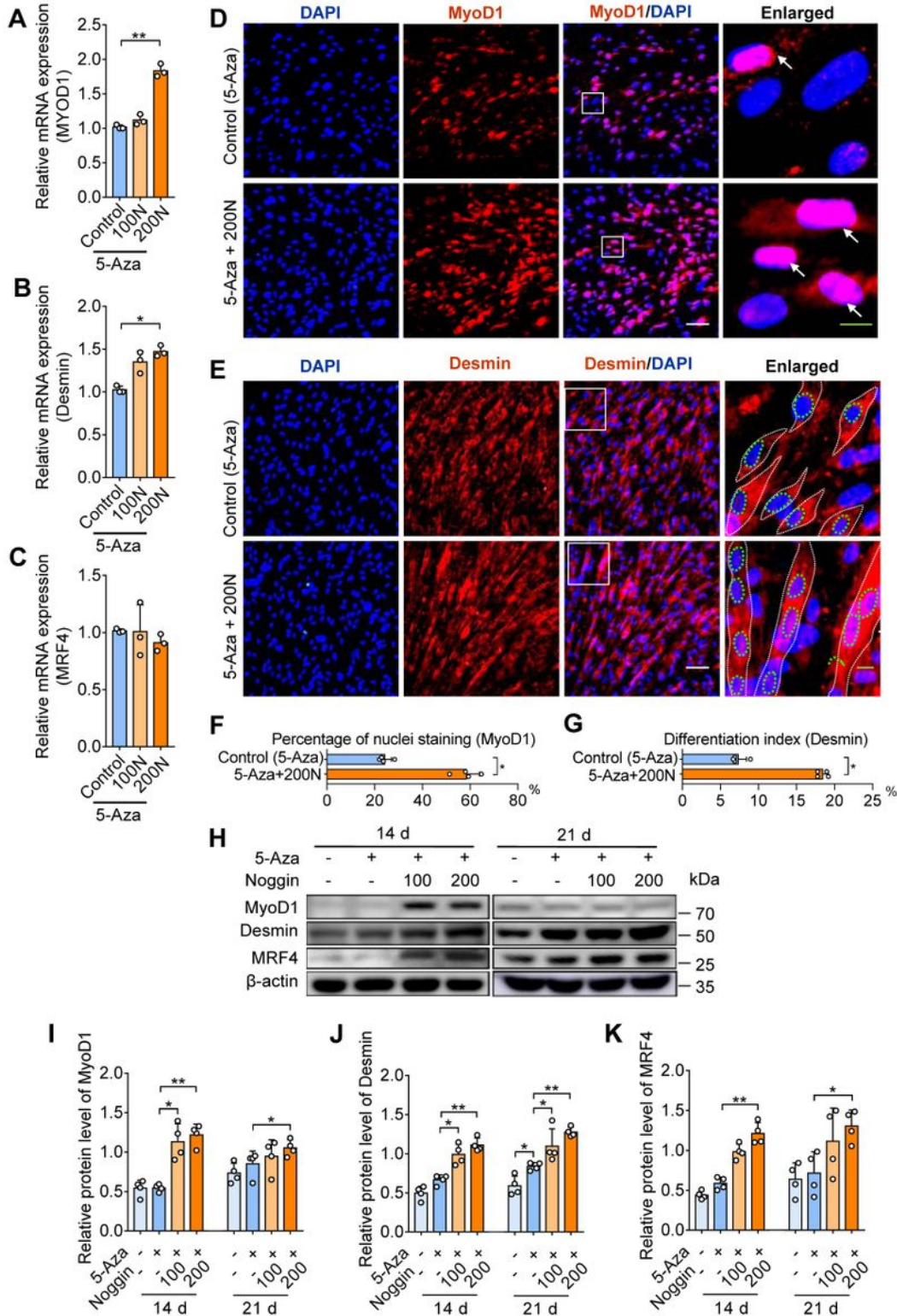


Figure 2

Noggin accelerates the progress of skeletal myogenic differentiation of DPSCs. A-C The levels of relative mRNAs, including (A) MyoD1, (B) Desmin, and (C) MRF4 were assessed using quantitative PCR (n = 3). D-E Immunofluorescence staining with MyoD1 (red) (D) or Desmin (red) (E) and DAPI (blue) on day 14 comparing 5-Aza induction with or without Noggin (200 ng/ml), respectively. Arrowheads indicate merged MyoD1 positive myonuclei; white dotted line indicated cell outline; green dotted circle indicated Desmin positive merged myonuclei; white scale bar, 50 μ m; green scale bar, 10 μ m. F Percentage of nuclei is presented as the ratio of MyoD1 positive nuclei to total nuclei (n = 4). G The differentiation index is presented as the ratio of Desmin positive nuclei to total nuclei (n = 4). H Protein expression of MyoD1, Desmin, and MRF4 was assessed using western blot on day 14 and 21. I-K Semiquantitative analysis of the expression ratio of (I) MYOD1/ β -actin, (J) Desmin/ β -actin, and (K) MRF4/ β -actin (n = 4). The differences between control and 5-Aza or between 5-Aza, 5-Aza + 100N and 5-Aza + 200N were presented as *p < 0.05, **p < 0.01 and ***p < 0.001. 100N = 100 ng/ml Noggin; 200N = 200 ng/ml Noggin.

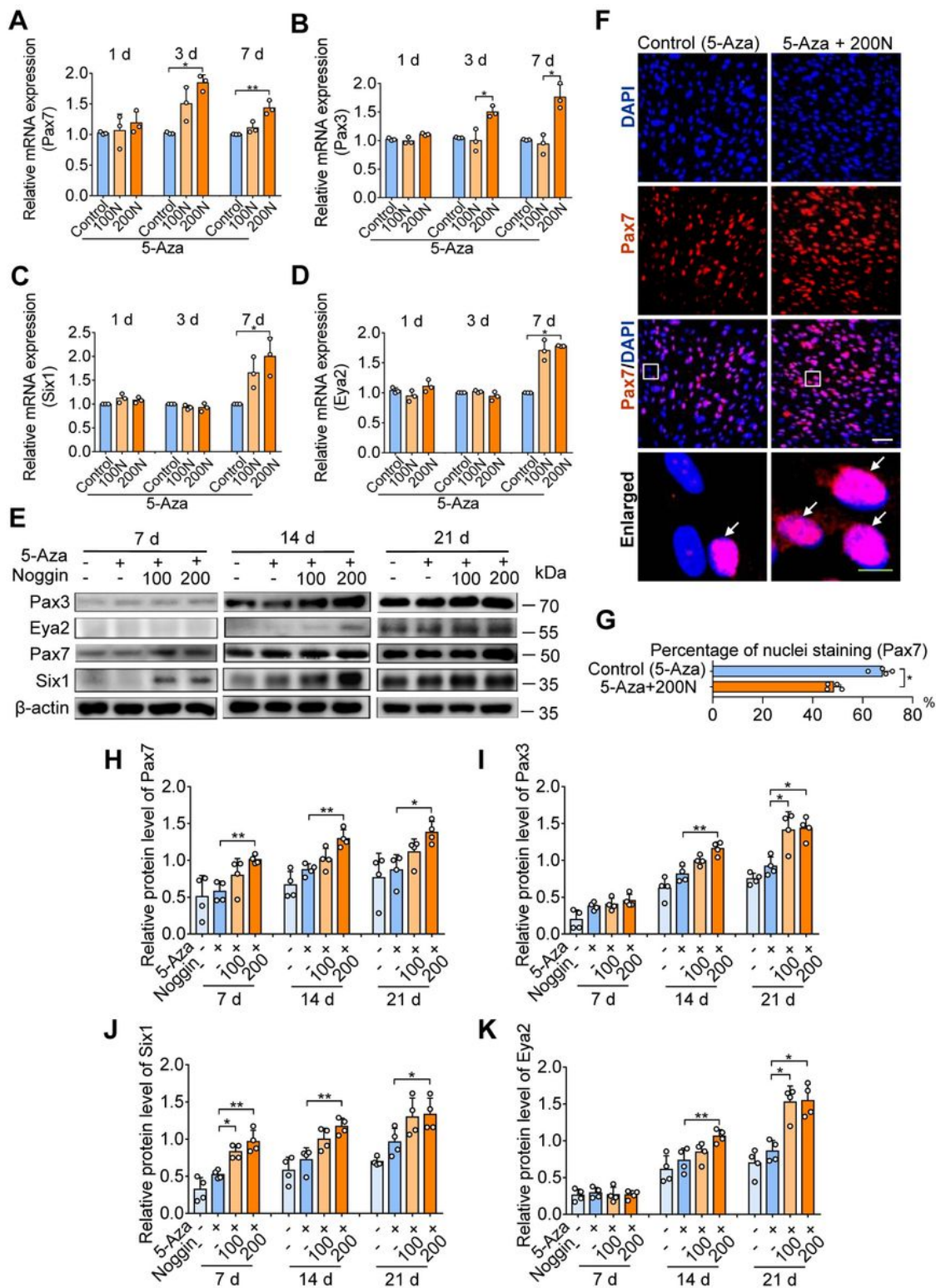


Figure 3

The generation of satellite-like cells in DPSCs and their asymmetric self-renewal capacity. A-D Relative mRNAs of (A) Pax7, (B) Pax3, (C) Six1, and (D) Eya2 were assessed on day 1, 3, 7 using quantitative PCR. E Protein expression of Pax7, Pax3, Six1, and Eya2 was assessed using western blotting on day 7, 14, and 21 (n = 3). F Immunofluorescence staining with Pax7 (red) and DAPI (blue) on day 14 comparing 5-Aza induction with or without Noggin (200 ng/ml), respectively. Arrowheads indicate merged Pax7

positive myonuclei; white scale bar, 50 μ m; green scale bar, 10 μ m. G Percentage of nuclei is presented as the ratio of Pax7 positive nuclei to total nuclei (n = 4). H-K Semiquantitative analysis of the expression ratio of (H) Pax7/ β -actin, (I) Pax3/ β -actin, (J) Six1/ β -actin, and (K) Eya2/ β -actin (n = 4) The differences between control and 5-Aza or between 5-Aza, 5-Aza + 100N and 5-Aza + 200N were presented as * p < 0.05, ** p < 0.01 and *** p < 0.001. 100N = 100 ng/ml Noggin; 200N = 200 ng/ml Noggin.

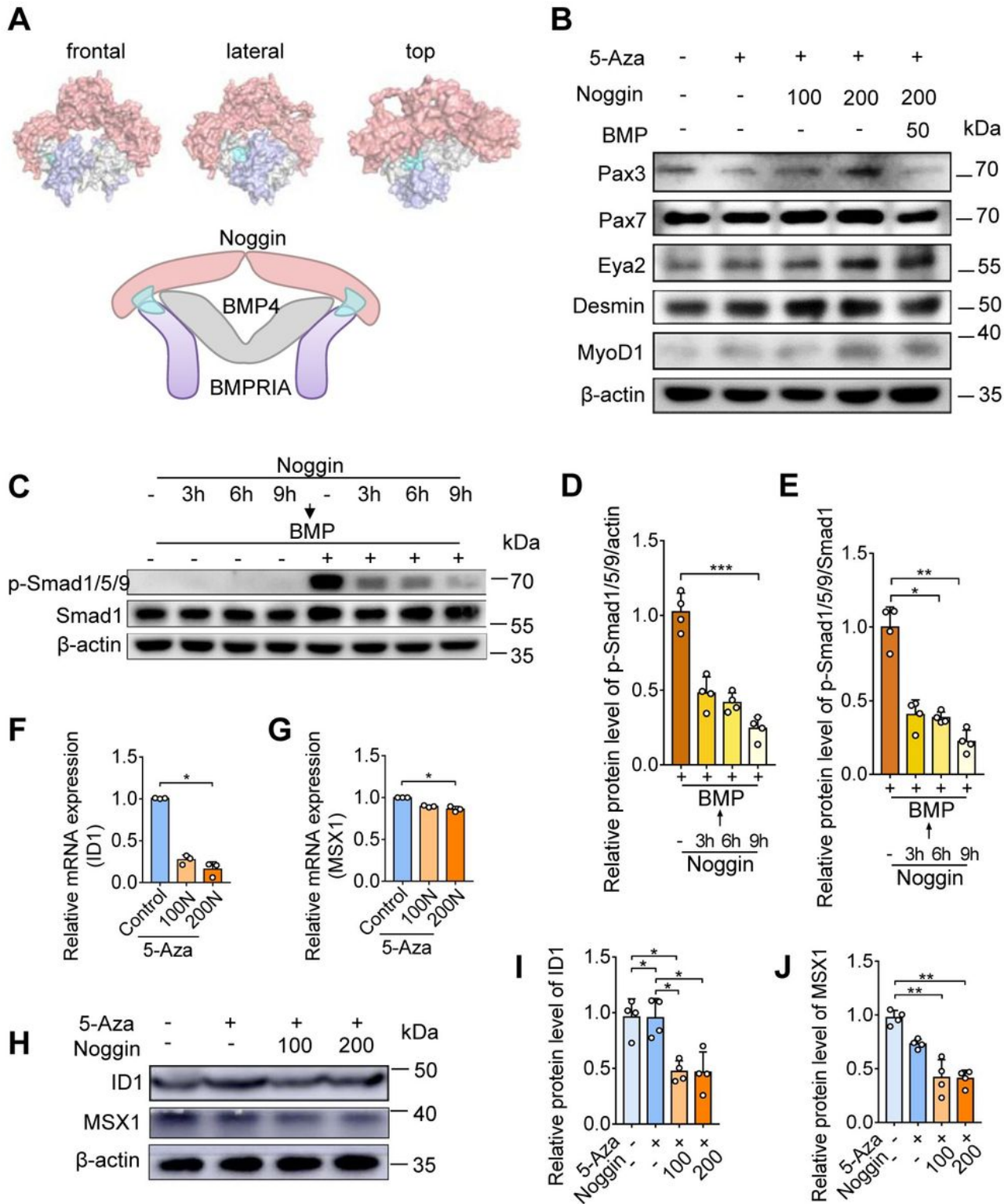


Figure 4

Noggin facilitates skeletal myogenic differentiation of DPSCs via Smad/Pax7 pathway. A 3D protein structure of Noggin's competitive inhibition of BMP4 binding to BMPRIA. Red indicate Noggin. Grey indicate BMP4. Purple indicate BMPRIA. Cyan indicate competitive site of Noggin binding to BMPRIA. B Protein expression of Pax7, Pax3, Eya2, MyoD1 and Desmin was assessed using western blot when rescuing with BMP4. C-E Protein expression of p-Smad1/5/9 and Smad1 was assessed using western blot by Noggin treatment for different times (3h, 6h, 9h) and subsequently stimulated with BMP4 or control for one hour (C), and semiquantitative analysis of the expression ratio of (D) p-Samd1/5/9/ β -actin, (E) p-Samd1/5/9/Smad1 were performed (n = 4). F-G relative mRNAs expression of (F) ID1 and (G) MSX1 were assessed using quantitative PCR (n = 3). H-J The protein expression levels (H) of ID1 and MSX1 were assessed using western blot, and semiquantitative analysis of the expression ratio of (I) ID1/ β -actin and (J) MSX1/ β -actin (n = 4). The differences between control and 5-Aza or between 5-Aza, 5-Aza + 100N and 5-Aza + 200N were presented as *p < 0.05, **p < 0.01 and ***p < 0.001. 100N = 100 ng/ml Noggin; 200N = 200 ng/ml Noggin

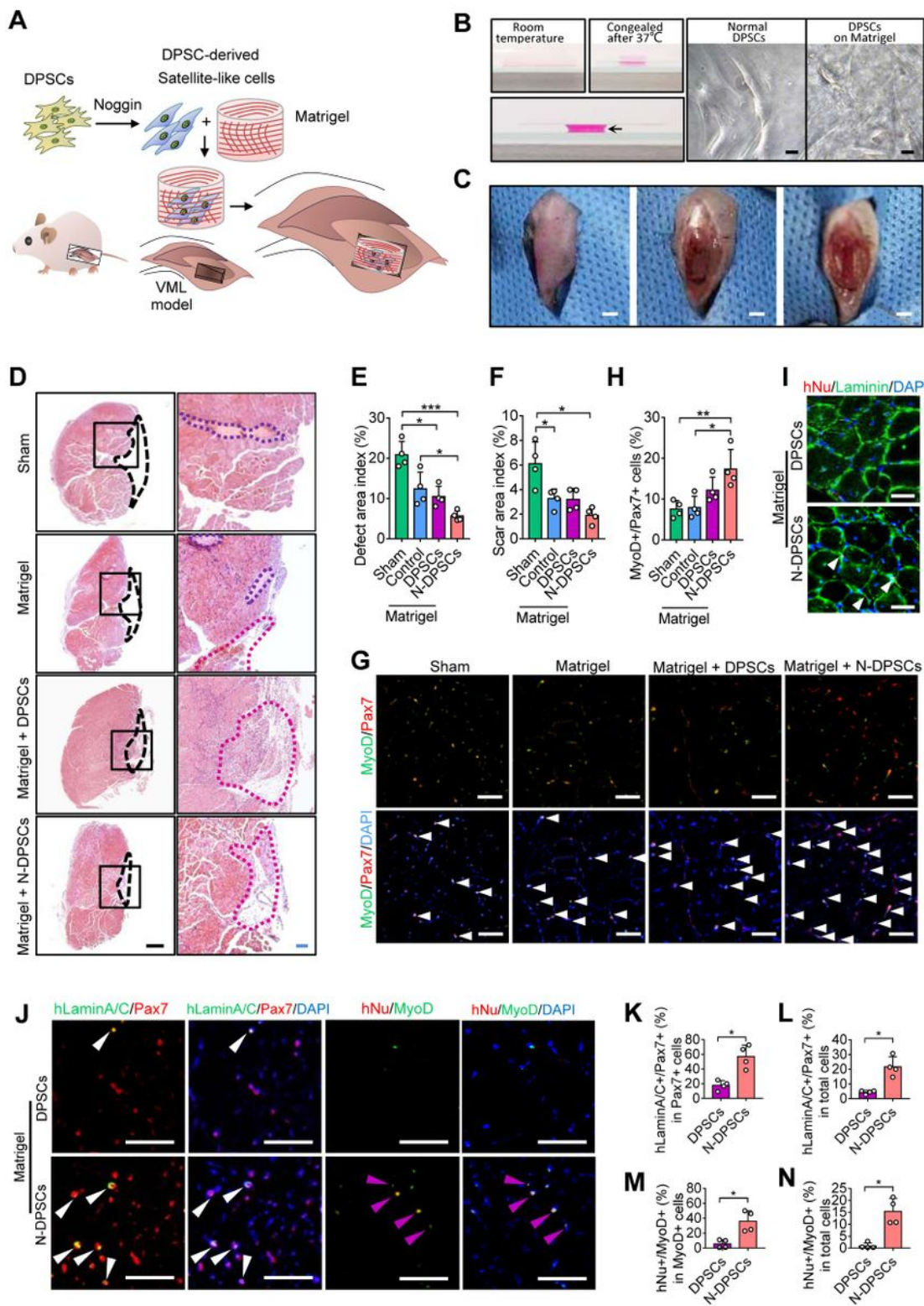


Figure 5

Noggin-pretreated DPSCs improved muscle repair on VML. A Schematic diagram of VML surgery, and transplantation of a bioconstruct containing cells and Matrigel into the TA muscle. B Characteristics of Matrigel at room temperature or congealed after 37°C (Left), and DPSCs cultured on common 96-well culture dish or Matrigel (Right). Arrowheads indicate space. Scar Bar, 10 μ m. C VML surgery. D H&E staining of TA muscle cross-sections. Large dotted black line indicated that the area removed in the

surgery but still remain defect; black box in the left column indicated the image area of right column; small dotted purple line indicated defect collagenous scar tissue; small dotted red line indicated repairing tissue infiltrated by diverse cells; black scale bar, 500 μm ; blue scale bar, 100 μm ; purple scale bar, 50 μm . E Defect area index was presented as the ratio of defect area to total muscle area ($n = 4$). F Scar area index was presented as the ratio of scar area to total muscle area ($n = 4$). G Representative Pax7 and MyoD immunostaining of muscle cross-sections. White arrowheads indicate Pax7+/MyoD+ cells. Scale bar, 20 μm . H Quantification of Pax7+/MyoG+ cells by immunofluorescence in muscle cross-sections ($n = 4$). I Grafted cells were identified by human Nucleoli (hNu) and by co-expression of hNu and Laminin. Arrowheads indicate hNu+ nuclear. Scale bar, 20 μm . J Donor-derived Pax7+ satellite-like cells were detected by human-specific LaminA/C and Pax7 co-immunostaining. Donor-derived MyoD+ myoblasts were detected by hNu and MyoD co-immunostaining. White arrowheads indicate hLaminA/C+/Pax7+ cells. Purple arrowheads indicate hNu+/MyoD+ cells. Scale bar, 20 μm . K-N Quantification of hLaminA/C+/Pax7+ in Pax7+ cells (K) or in total cells (L), and hNu+/MyoD+ in MyoD+ cells (M) or in total cells (N). The differences were presented as * $p < 0.05$, ** $p < 0.01$ and *** $p < 0.001$. VML = volumetric muscle loss; N-DPSCs = Noggin-treated DPSCs.

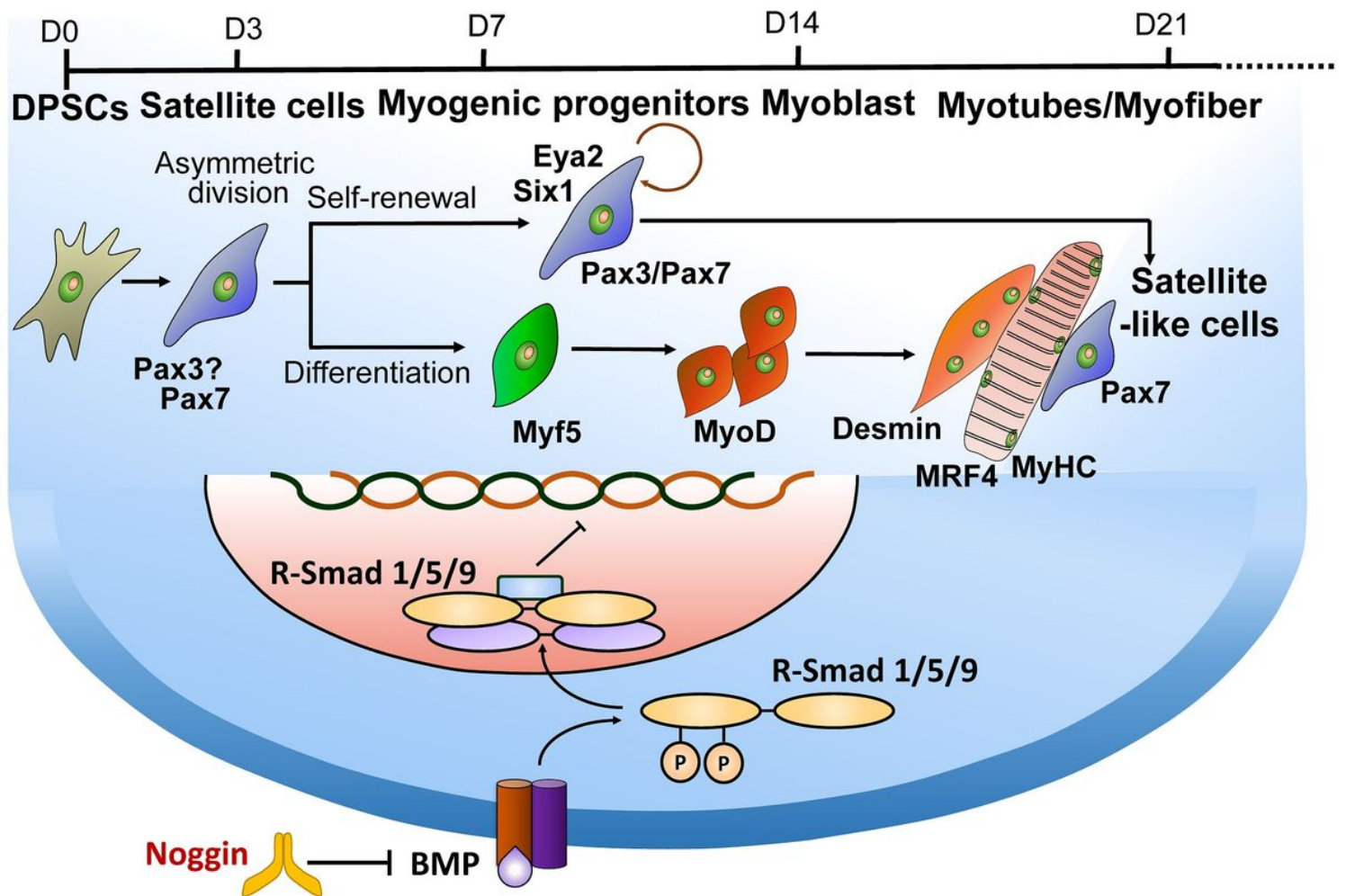


Figure 6

The possible mechanism of Noggin regulating the myogenic differentiation of hDPSCs. Noggin regulates BMP pathway by regulating the phosphorylation of Smad 1/5/9, so as to promote the myogenic differentiation of dental pulp stem cells. This way of differentiation preserves the asymmetric self-renewal and commitment of Pax7+ satellite-like cells in DPSCs. Diagram mapping the developmental stages of myogenic differentiation from hDPSCs was also described above, accompanied by a time line of myogenic markers.

Supplementary Files

This is a list of supplementary files associated with this preprint. Click to download.

- [ZhangetalSupplymentalMaterial.docx](#)
- [GraphicAbstract.tiff](#)